Supporting Information

Resonance loss due to polarization accumulation effect induced by phosphorus vacancies for enhancing electromagnetic wave absorption

Shaoyao Tian, Zhihao Sun, Han Ding, Zihao Guo, Peng Wang, Yu Qiu, Benli Du, Lei Qian*

Key Laboratory for Liquid-Solid Structural Evolution and Processing of Materials (Ministry of Education), Shandong University, 17923 Jingshi Road, Jinan, 250061, China

*Corresponding author, Email address: qleric@sdu.edu.cn (Lei Qian).

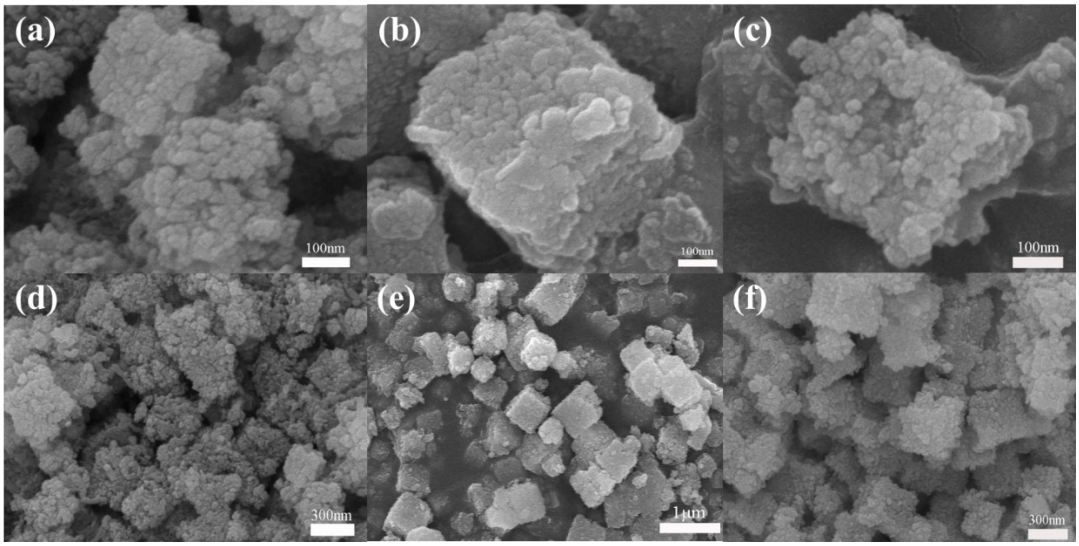

Fig. S1. FESEM images of (a, d) Pv40-CoP@C, (b, e) Pv50-CoP@C, (c, f) Pv60-CoP@C.

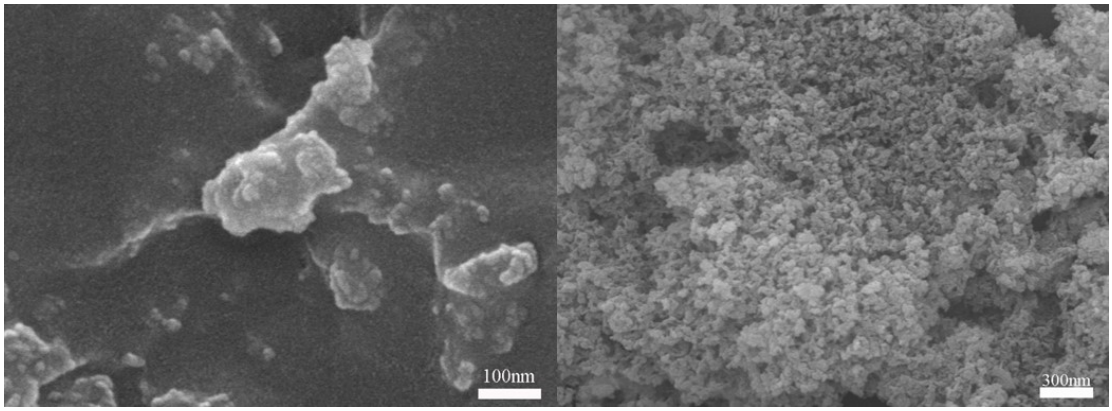

Fig. S2. FESEM images of Pv120-CoP@C.

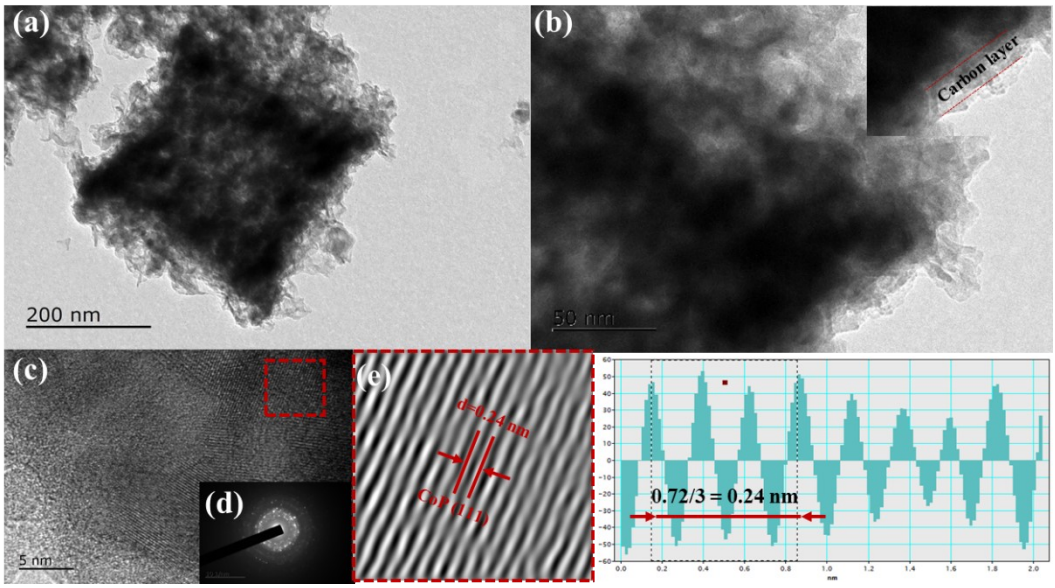

Fig. S3. (a, b) TEM images of Pv50-CoP@C nano-cube. (c) HRTEM image of Pv50-CoP@C nano-cube. (d) SAED pattern of Pv50-CoP@C nano-cube. (e) Lattice spacing diagram of Pv50-CoP@C

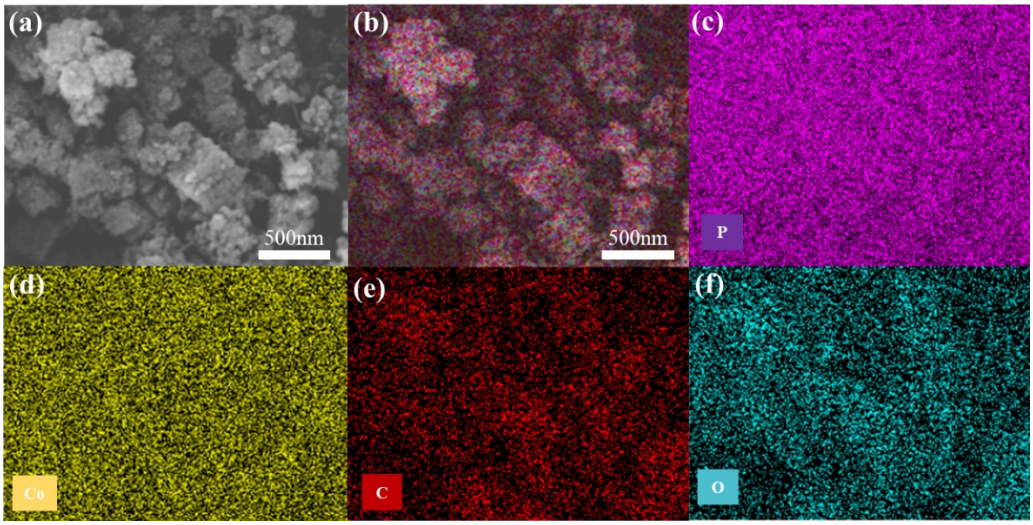

Fig. S4. Image of element distribution of Pv60-CoP@C.

Table S1 The elemental content of Pv60-CoP@C

Element	Apparent concentration	Wt %	Atomic percent
C	13.47	33.52	57.81
N	0.73	0.40	0.60
O	25.04	13.49	17.46
P	54.56	17.79	11.90
Co	62.93	34.80	12.23
Gross amount		100.00	100.00

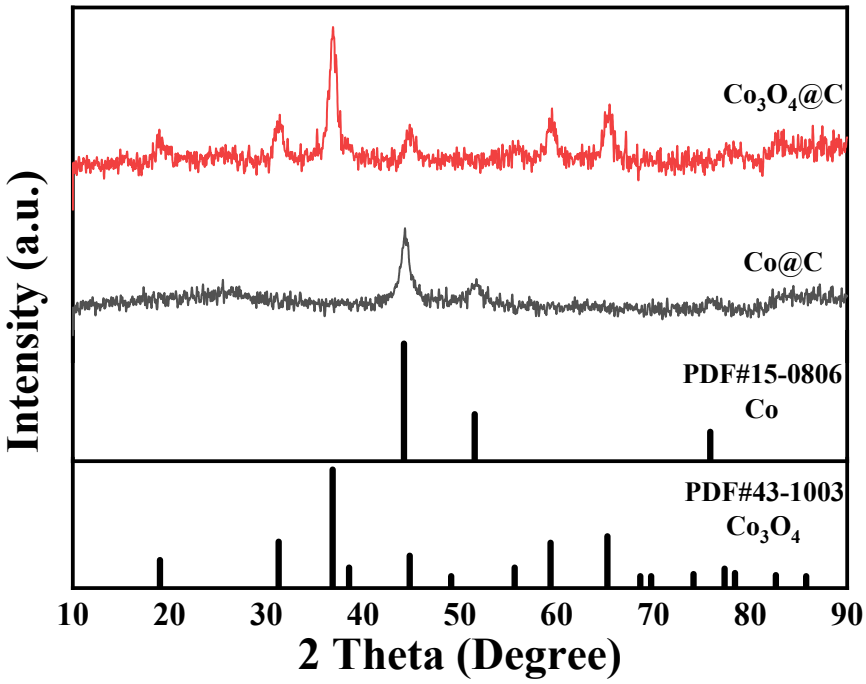

Fig. S5. XRD pattern of Co@C and Co_3O_4@C.

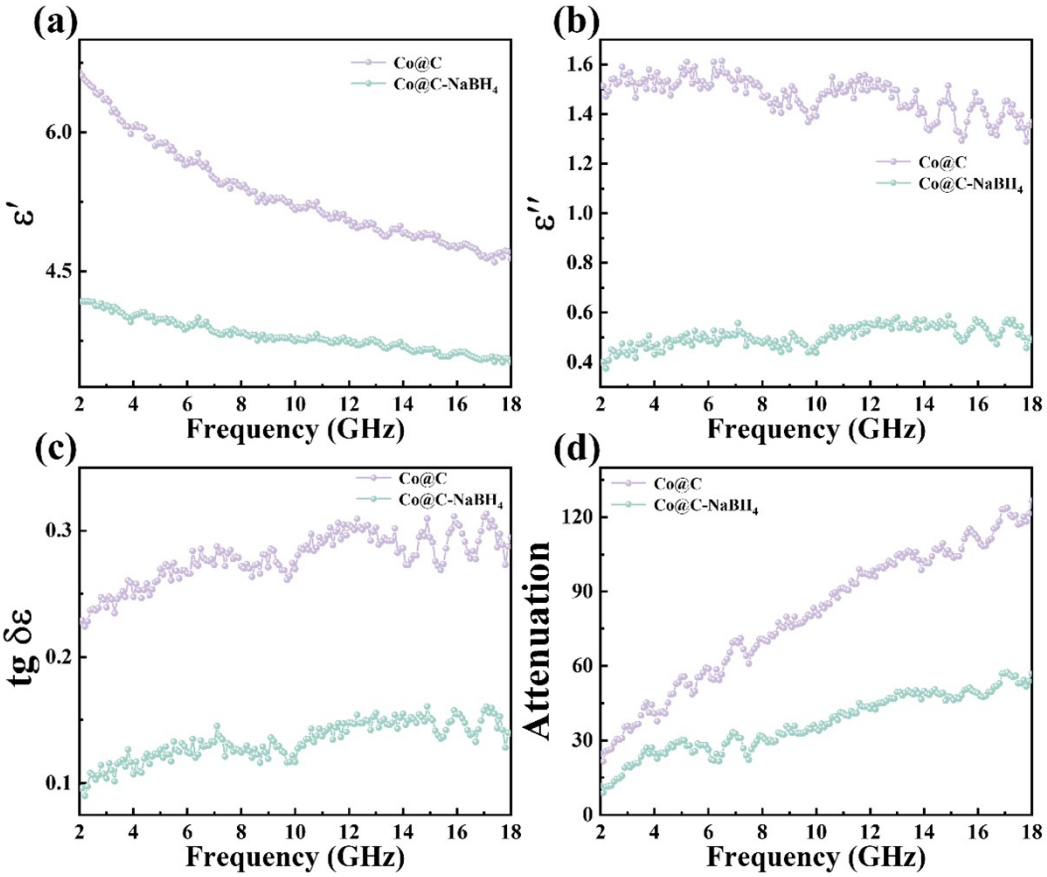

Fig. S6. (a) The dielectric real part, (b) dielectric imaginary part, (c) dielectric loss tangent, (d) attenuation of Co@C and Co@C-$NaBH_4$.

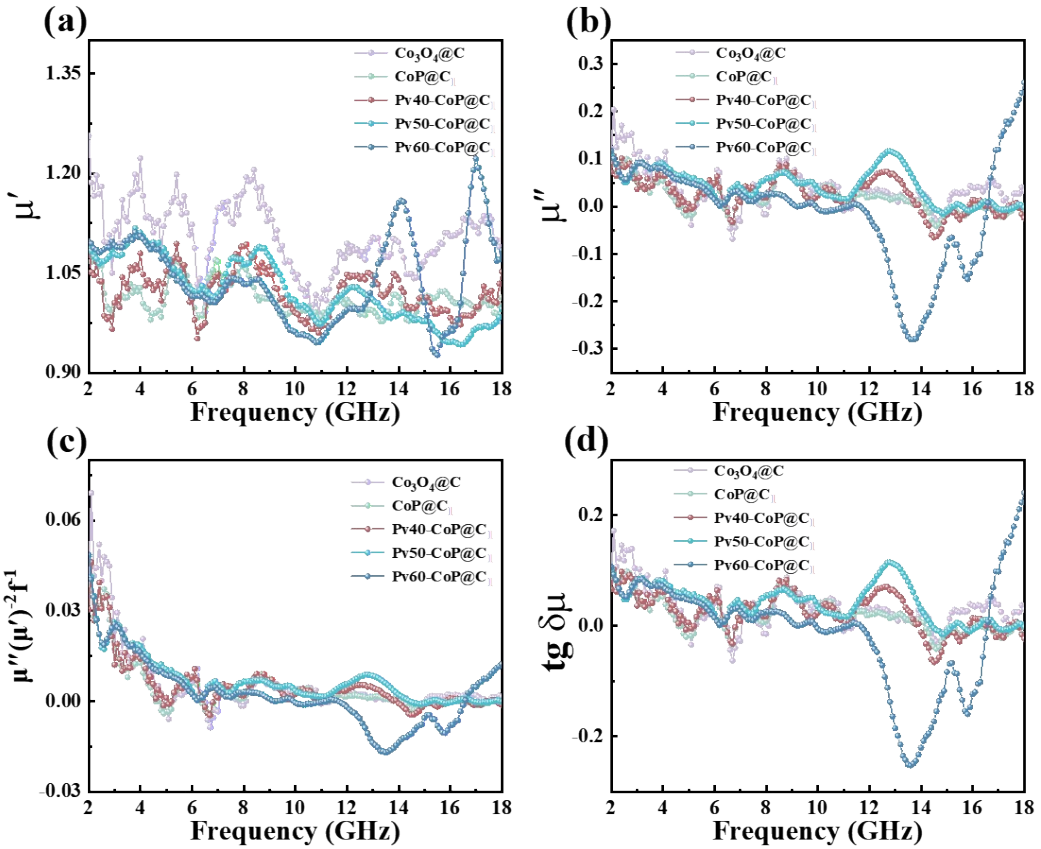

Fig. S7. (a) The real part of permeability, (b) imaginary part of permeability, (c) frequency-dependent $\mu''(\mu')^{-2}f^{-1}$ curves and (d) tan $\delta\mu$ value of Co_3O_4@C, CoP@C, Pv40-CoP@C, Pv50-CoP@C and Pv60-CoP@C.

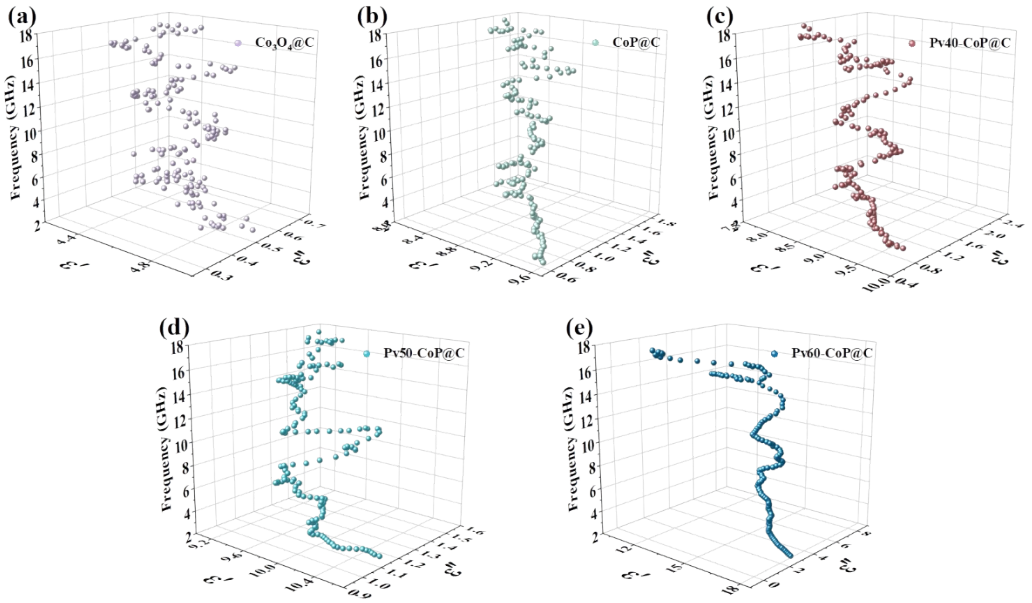

Fig. S8. Cole-Cole curves of (a) Co_3O_4@C, (b) CoP@C, (c) Pv40-CoP@C (d) Pv50-CoP and (e) Pv60-CoP@C.

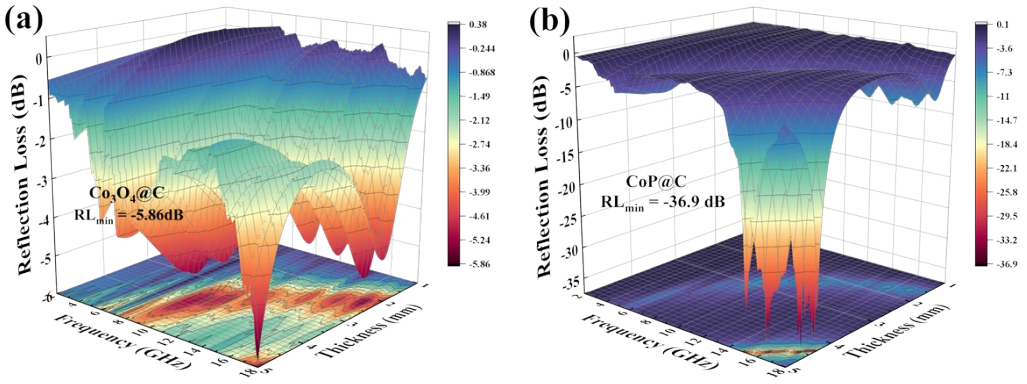

Fig. S9. The 3D RL_{min} diagram of (a) Co_3O_4@C, (b) CoP@C.

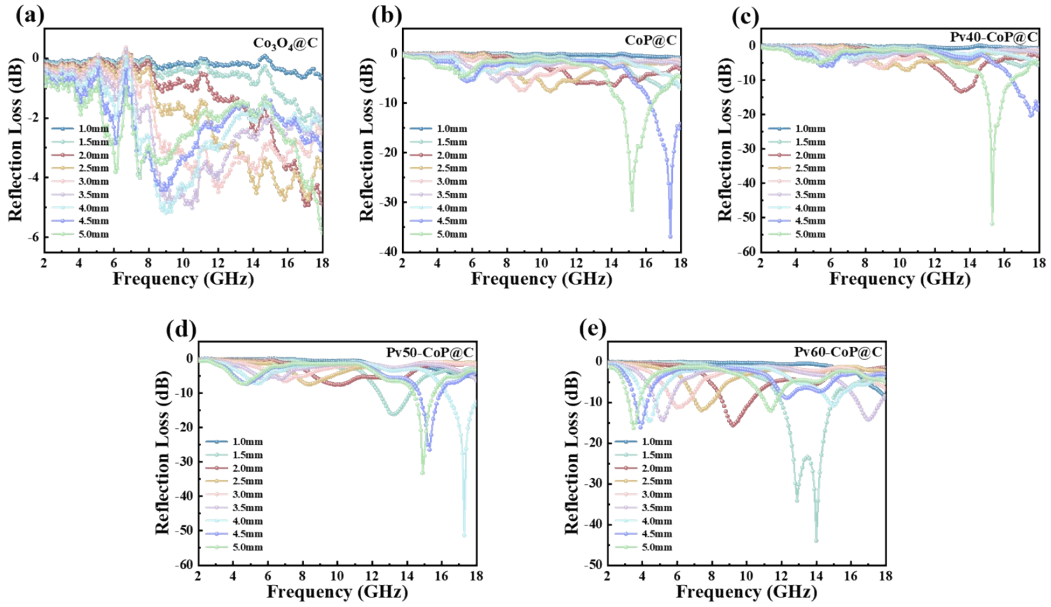

Fig. S10. The 2D RL_{min} diagram of (a) Co_3O_4@C, (b) CoP@C, (c) Pv40-CoP@C, (d) Pv50-CoP@C and e Pv60-CoP@C.